

# Experimental research of the impact of upper reinforcement on the tension membrane action of narrow three-span reinforced concrete slabs

Mirosław Wieczorek<sup>1</sup>

<sup>1</sup>Silesian University of Technology, Faculty of Civil Engineering, Gliwice, Poland

**Abstract.** The aim of the paper was to demonstrate the influence of reinforced steel parameters and quantity on the failure mechanism of four three-span models of reinforced concrete strips with the dimensions 7140×500×190 mm. Two models had only bottom reinforcement, while two were reinforced at the bottom and upper sides. The paper contains the description of the experimental stand and models along with the results of experimental tests which were compared with the results of the calculations based on traditional methods.

## 1 Introduction

The experimental research discussed in the article is the follow-up of the investigations of the behavior of narrow reinforced concrete slabs in an emergency situation induced by overloading [9, 10]. The most common reason of overloading in slab structures is the improper operation of a building which results e.g. from the excessive load exerted on parts or entire surfaces of floors. The second reason of overloading are the faults made at the design stage (e.g. improperly defined amount of reinforcement) or during the construction of buildings (e.g. supplying the concrete of incorrect strength parameters), resulting in damaging of the structure even with the correct value of load. The purpose of the research was to determine the maximum value of the load that the reinforced concrete slab will be able to carry due to the membrane work, which appears in continuous elements in the event of even a slight vertical displacement. The first works in the field of the membrane work were carried out by Park (1964) [8], followed by Black (1975) [4], Desaya and Kulkarnia (1977) [5] as well as Hawkins and Mitchell (1979) [6]. Based on the analysis literature, the summary was made by Mitchell and Cook (1984) [7]. However, the above-mentioned works were performed on spatial models, which hinders conducted the analysis. An analysis of narrow slabs working in one direction was proposed to partially simplify the first approach to recognizing the problem. The paper presents the results of the research of two models with the dimensions of 7140×500×190 mm, where upper support reinforcement was applied. Such a method of reinforcing is commonly applied in engineering practice.

## 2 Description of the experimental models

Similarly to papers [9, 10], the test models have been designed as narrow slabs of a typical slab-column structure with unidirectional reinforcement. In order to conduct the tests, two identical models with the shape of a flat reinforced concrete slab with the dimensions of 7140×500×190 mm (Fig. 1) have been constructed. Similarly to papers [9, 10], it has been assumed that the length of the tested part of the slab would exceed the height of the cross-section ca. 30 times. In order to reinforce the models, bars with a diameter of 12 mm were used (no. 1 in Fig. 1), made from class C steel according to [3]. The reinforcement ratio was (Model 1 -  $\rho = 1.0\%$ , Model 2  $\rho = 2.0\%$ ). As a transverse reinforcement, bars with a diameter of 8 mm (no. 2 in Fig. 1) made from class C steel according to [3] were used. The models, apart from the bottom reinforcement, also feature upper reinforcement with the same number of bars (Fig. 1). View of the bottom and upper reinforcement can be found in Fig. 2. Prior to concreting, the bottom reinforcement was welded to steel plates (no. 3 in Fig. 3). In the last stage of the preparatory works, steel plates were immobilized in the test stand (Fig. 4). The model was built using concrete compound based on the formula identical to research [9, 10].

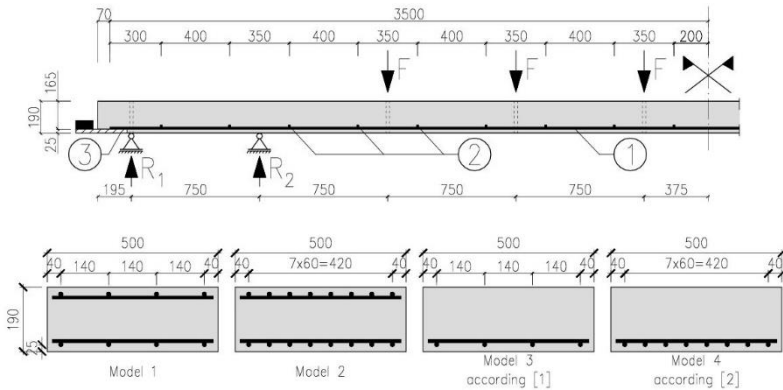


Fig. 1. Model of testing - arrangement of the reinforcement.

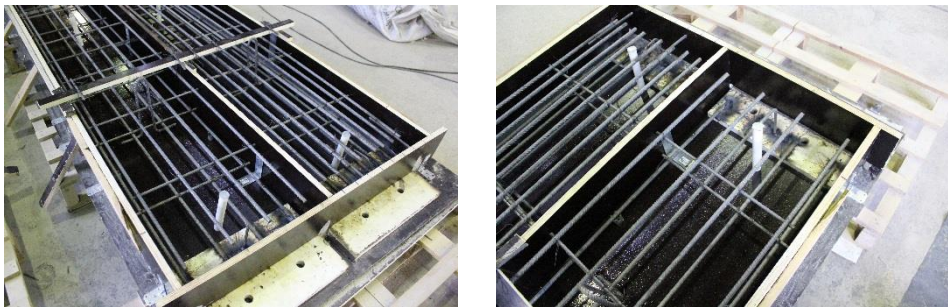
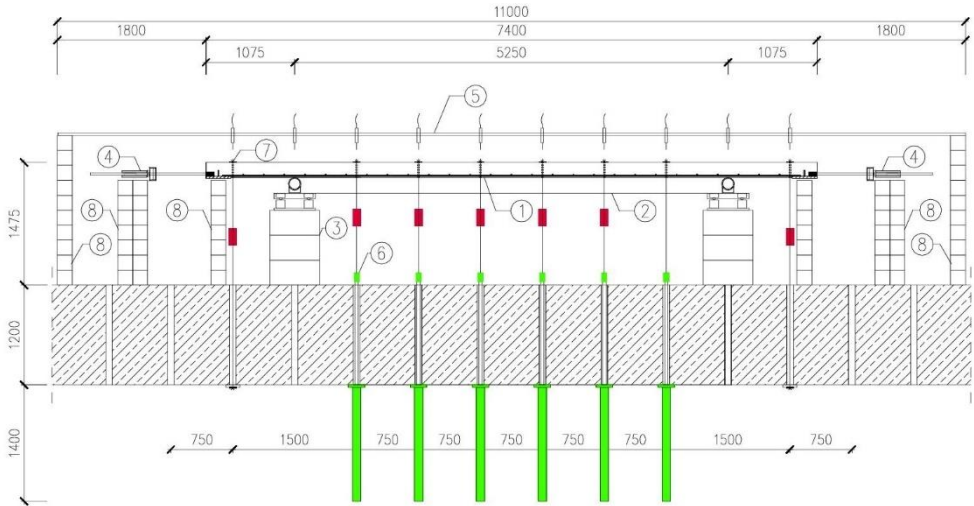


Fig. 2. View of reinforcement.

## 3 Description of the test stand

The test stand on which the research models were arranged consisted of two supports allowing to slide and turn the slab (no. 2 in Fig. 3) placed on concrete blocks (no. 3 in Fig. 3) with a spacing of 5250 mm. In order to stabilize the model during the research and afterwards,

additional supports were placed on its ends (no. 8 in Fig. 3) – supports R1 and R4. The model was loaded with the set of 18 hydraulic actuators (no. 6 in Fig. 3) arranged in six measurement points. Compared to the research [9, 10], actuators with better parameters were used, allowing to carry out the tests until the reinforcing bars were ruptured. The displacements were measured using eleven sensors placed every 750 mm (no. 6 in Fig. 3). The horizontal interlocking of the model was made of two horizontally arranged sheets (no. 4 in Fig. 3, Fig. 4a) locked with steel angle struts.



**Fig. 3.** The test stand according to [9, 10] (1- test model; 2- articulated sliding support allowing to slide and turn the model simultaneously; 3- concrete base of the articulated support; 4- horizontal model stabilization system; 5- inductive sensors to measure the vertical displacements of the upper surface in the tested models; 6- model load system consisting of six sets of hydraulic cylinders; 7- vertical reaction R1 and R4 measuring system; 8- auxiliary items supporting the ends of the test model).



**Fig. 4.** Photos of selected parts of the stand: a) horizontal interlocking scheme, b) articulated sliding support, c) the entire model.

## 4 Description of the research methodology

Similarly to [9, 10], the same procedure was applied in the tests of each analyzed model. The test program consisted of the following four stages:

- Stage 0: This stage of tests included: placing the model on the supports, reading the support reactions, determining the weight of the element, static calculations of the proper distribution of the support reactions, rectification of the model on supports, and blocking the horizontal displacements of the tested element ends.

- Stage 1: The initial loading of the model with a horizontal force of  $H1 = H2 = 6$  kN was aimed at adjusting the measurement system to the model and the test stand. After the first loading cycle the measuring apparatus was reset and the actual course of the test began.
- Stage 2: A single loading cycle included applying a load on the tested model to the value equal to 10% of the design load that determines flexural destruction of a given element.
- Stage 3: The consecutive loading cycles were applied on the tested model until the moment of its flexural destruction.
- Stage 4: The final stage of the tests included a single loading cycle of the test model until the moment of its total failure resulting from the rupture of the reinforcement bars.

## 5 Materials

The reinforcement of the models consisted of bars made of medium ductility steel of class C according to [3] ( $1.15 < f_{tk}/f_{yk} < 1.35$ ). The results of testing the steel have been collected in Table 1. The models were constructed of concrete based on Portland cement and aggregate with the diameter of the grains up to 8 mm. On the day of testing, i.e. after 32 days of concrete curing, the mechanical parameters were determined in compliance with PN-EN 12390-3:2011 [1, 2] standard. Table 2 contains the mean values of the mechanical parameters which were always determined on six samples. Although the compound used was identical to the one applied in tests [9, 10], the parameters of the obtained concrete differed slightly.

**Table 1.** Mechanical parameters of rough bars, tested in compliance with PN-EN 10002-1:1998.

Diameter of the bar $\phi$ [mm]	Module of elasticity $E$ [GPa]	Yield strength $f_{yk}$ [MPa]	Tensile strength $f_{tk}$ [MPa]	Total elongation at maximum force $\epsilon_{uk}$ [%]
8	191.852	526.8	604.4	14.91
12	199.242	601.2	714.2	11.8

**Table 2.** Mechanical parameters of concrete investigated in compliance with PN-EN 12390-3:2002.

Module of elasticity $E_{cm}$ [GPa]	Compressive strength $f_{c,cyl}$ [MPa]	Compressive strength $f_{c,cube}$ [MPa]	Tensile strength $f_{cm}$ [MPa]
34.81	34.22	44.10	3.77

## 6 Results of the laboratory tests

In the course of the research, the loading force was measured along with the corresponding vertical displacement in the centre of the span of the investigated slab (Fig. 5 and Fig. 6), and the image of the emerging cracks was prepared. Detailed values of displacements and loads are presented in Table 3. In order to determine the impact of the upper reinforcement on the load-bearing capacity of the tested models, Table 3, Fig. 5 and Fig. 6 contain results obtained for models with the same amount of bottom reinforcement: Model 3 according to [9] and Model 4 according to [10].

In the course of the research and in papers [9, 10], the hydraulic loading system was applied, where in the case of a violent deformation of the test element the pressure in the hydraulic system decreases, causing a partial discharge of the test model. Fig. 5 and Fig. 6 include markings of points where a temporary discharge of elements occurred as a result of concrete crushing.

**Table 3.** Characteristic load values with the corresponding vertical displacements.

Stage of the element action	Load value [kN / loading set]				Deflection of model [mm]			
	Model 1	Model 2	Model 3 [9]	Model 4 [10]	Model 1	Model 2	Model 3 [9]	Model 4 [10]
before the destruction of top reinforcement	destruction of the first bar 20.3				destruction of the first bar 502			
	destruction of the second bar 25.2	all bars lost bonding 28.44	-	-	destruction of the second bar 615	59.35	-	-
	destruction of the third and fourth bar 26.3				destruction of the third and fourth bar 630			
after the destruction of top reinforcement		14.24			63.04			
before the flexural destruction	17.99	46.95	8.47	16.15	396.15	369.18	277.4	221.3
after the flexural destruction	14.73	42.16	4.8	12.1	412.9	375.78	281.4	233.0
before completing the tests	51.86	97.21	31.2	52.25	608.65	769.65	558.7	530.12

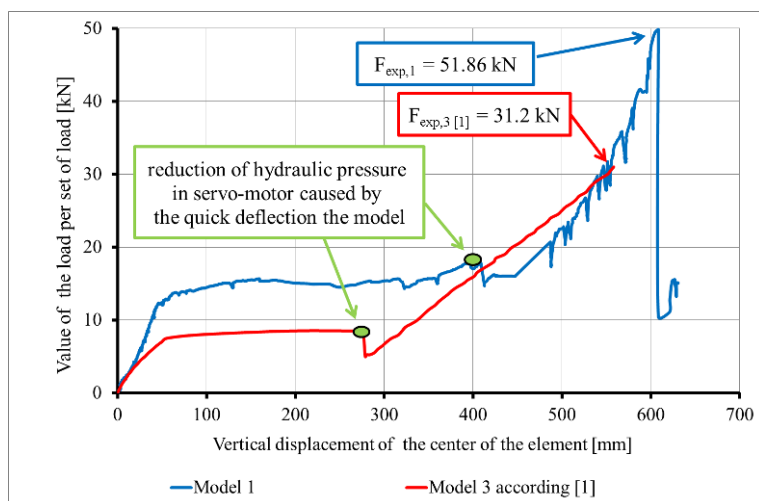


**Fig. 5.** Results - displacement of the center of the Model 1 and Model 3 as a function of load.

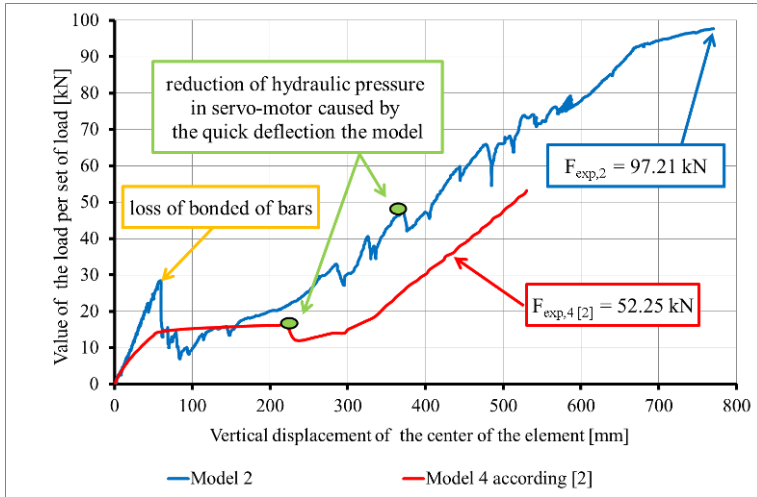


**Fig. 6.** Results - displacement of the center of the Model 2 and Model 4 as a function of load.

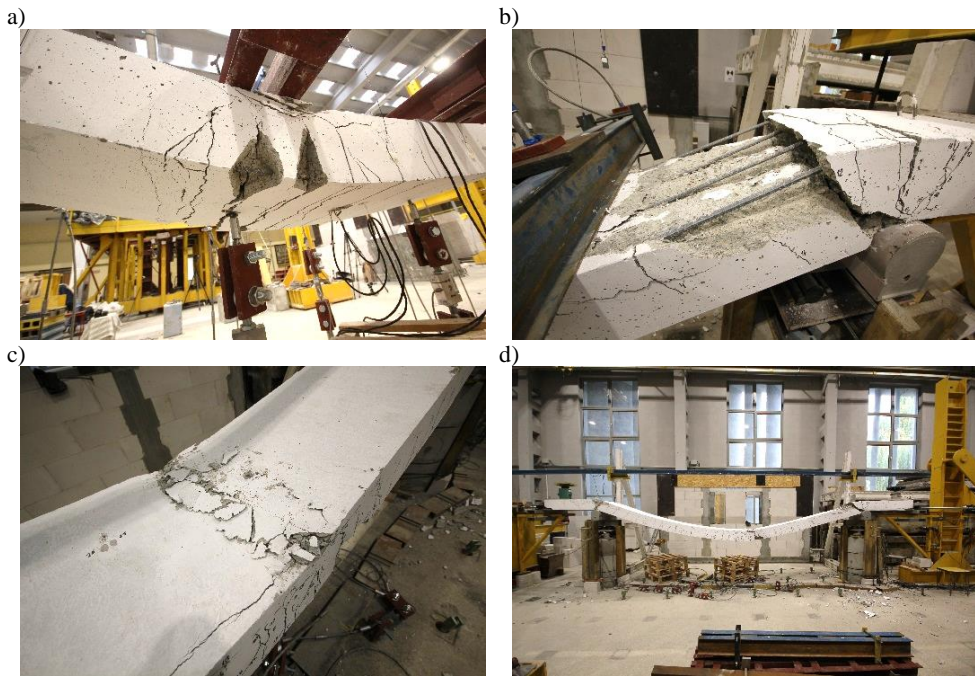


**Fig. 7.** Photos of the model during the tests Model 1 (examples): a) cracks centre of the model, b) crack over the R3 support, c) spalling of concrete in the centre of the model span, d) view of the model after the tests.

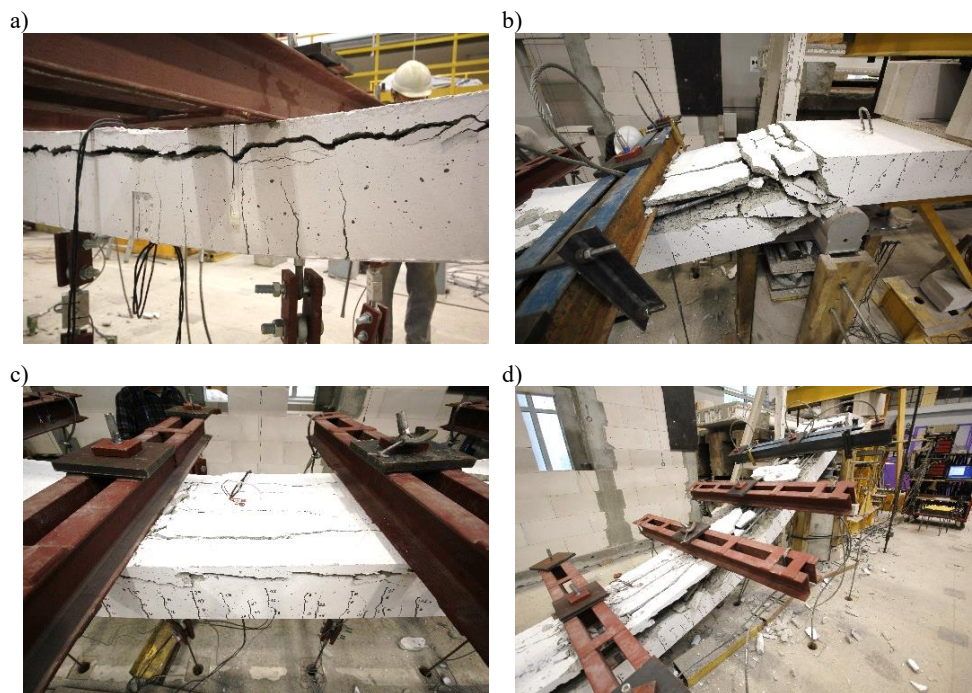


**Fig. 8.** Photos of the model during the tests Model 2 (examples): a) cracks centre of the model, b) crack over the R3 support, c) spalling of concrete in the centre of the model span, d) view of the model after the tests.

## 7 Determination of theoretical values of failure loads

Theoretical values of failure loads causing the flexural destruction of the models have been determined according to [3], taking into account geometrical and material details of the models. Table 4 includes both the values of experimental and calculation load:

1 - theoretical design value of variable load (exceeding the dead weight of the element), taking into account the safety and material coefficients, at which flexural destruction of the element should occur

Calculations were carried out according to [3]. In the calculations, it was assumed that the load-bearing capacity of models with bottom and both bottom and upper reinforcement would be determined solely taking into account the bottom reinforcement.

2 - theoretical characteristic variable load (exceeding the dead weight of the element) at which flexural destruction of the element should occur

Calculations were carried out according to [3]. The value of load was determined with the assumption that all safety coefficients equal 1.0.

3 - theoretical characteristic variable load (exceeding the dead weight of the element) at which tensioning destruction should occur

The value of load has been determined in a way applied for a perfect tension member with the following calculation assumptions [9, 10]:

- the shape of tension member axis deflection is determined with the formula of the catenary curve;
- the length  $l'$  of the tension member after deformation in the failure state is equal to the initial length increased by the percentage elongation  $A_{gt}$  determined on the basis of material tests of steel;

- the value of horizontal reaction H equals the force transferred by the reinforcing bars.
- 4 - experimental value of load (exceeding the dead weight of the element) at which flexural destruction of the element occurred
- 5 - experimental value of load (exceeding the dead weight of the element) at which research was interrupted due to technical reasons
- 6 - experimental value of load (exceeding the dead weight of the element) at which reinforcing bars were ruptured

**Table 4.** Theoretical and experimental load values (values in kN).

Type of load	Model 1	Model 2	Model 3 [9]	Model 4 [10]
1. Theoretical design value of variable load (exceeding the dead weight of the element) taken into account in the strip design	3.0	6.0	3.0	6.0
2. Theoretical characteristic variable load (exceeding the dead weight) at which flexural destruction should occur	7.9	14.06	7.9	14.06
3. Theoretical characteristic variable load (exceeding the dead weight of the element) at which tension destruction should occur	59.5	105.89	59.5	105.89
4. Load at which flexural destruction of the models occurred (crushing of the compressed concrete zone)	17.99	46.95	8.47	16.15
5. Load at which the research was completed without the total failure of the models	-	-	31.2	52.25
6. Load at which the research was completed with total failure of the models	51.86	97.21	-	-

## 8 Analysis of the results

The research led to the following conclusions:

- In each tested model, a uniform image of cracking with significant apertures of cracks was obtained on lateral surfaces, which points at substantial yielding of the reinforcement and high influence of steel ductility on the possibility of a local redistribution of internal forces. What is more, at the moment of failure of Model 1 and Model 2 very high slab deflections were obtained (608 mm - Model 1 and 770 mm - Model 2 respectively). The proportion of deflection in relation to the slab span equalled  $a/l = 1/8.61$  in Model 1 and  $a/l = 1/6.82$  in Model 2.
- The values of load at which flexural failure of the element occurred in the course of the research (4 according to Table 4) with Model 3 and Model 4 were close to theoretical characteristic values of the load (2 according to Table 4). The comparison of the same load values with Model 1 and Model 2 exhibited a significant impact of upper reinforcement on the load-bearing capacity of the compressed slab zone. Values obtained in the course of the research of Model 1 and Model 2 were over 2 times higher than the theoretical values.
- As predicted, failure of the support zone in Model 1 occurred at R2 support. As a result of rupturing the reinforcing bars, a plastic hinge emerged, and the model started to operate in a way identical to a model with bottom reinforcement bars only. In Model 2, a plastic hinge also emerged over R2 support, induced by the loss of adhesion of all upper reinforcement bars.

- All tested models displayed an identical failure mechanism consistent with the applied methodology of research and the following preliminary assumptions:
  - horizontal interlock of the model beyond the load impact zone – lack of horizontal displacements,
  - emergence of plastic hinges over R2 and R3 supports – following the above description in Model 1 and Model 2 and directly after applying the load in Models 3 and Model 4.
- The application of a new loading system made it possible to obtain the value of load at which reinforcing bars in Model 1 and Model 2 were ruptured. The following values of loads were obtained:
  - about 17.29 and 16.2 times higher than the value of load with regard to which Model 1 and Model 2 were designed (value of force - 1 according to Table 4),
  - about 6.56 and 6.91 times higher than the value of load with regard to which Model 1 and Model 2 were designed (value of force - 2 according to Table 4),
  - about 87.2% and 91.8% of the theoretical load-bearing capacity utilization with regard to tensile membrane action of the element (value of force - 3 according to Table 4).

## 9 Summary

The presented experimental research was mainly aimed at observing the behavior of models and the emerging damages when both upper and bottom reinforcement were applied. Introducing the new method of loading the models made it possible to experimentally define the load-bearing capacity of the tested models with regard to tensile membrane actions. The values of failure load of the models obtained in the course of the research clearly pointed at very high reserves of the load-bearing capacity resulting from this type of operation exhibited by a reinforced concrete element.

## References

1. EN 12390-3:2011 Concrete Tests - Part 3: The compressive strength of test samples (2011)
2. EN 12390-6:2011 Testing Hardened Concrete - Part 6: Tensile splitting strength of test specimens (2011)
3. EN 1992-1-1:2004/AC, Eurocode 2: Design of concrete structures – Part 1-1: General rules and rules for buildings (2010)
4. M.S. Black: *Journal of the Structural Division*, **101**, No. ST1 (1975)
5. P. Desayi, A.B. Kulkarni: *Materials and Structures*, **10**, 59 (1977)
6. N.M. Hawkins, D. Mitchell: *ACI Journal*, **76**, 10 (1979)
7. D. Mitchell, W.D. Cook: *Journal of Structural Engineering*, **110**, 7 (1984)
8. R. Park: *Magazine of Concrete Research*, **16**, 40 (1964)
9. M. Wiczorek: *Solid State Phenomena*, **240** (2015)
10. M. Wiczorek: *Procedia Engineering*; **190** (2017)